Two-dimensional Numerical Simulation of a Pulsed Heat Source High Temperature Inert Gas Plasma MHD Electrical Power Generator

Masaharu Matsumoto, Tomoyuki Murakami and Yoshihiro Okuno
Department of Energy Sciences, Tokyo Institute of Technology
4259-G3-38 Nagatsuta-cho, Midori-ku, Yokohama 226-8502, Japan
d06matsumoto@es.titech.ac.jp

Keywords: Magnetohydrodynamics, Inert gas plasma, Electrical power generation

Abstract

Performance of a pulsed heat source high temperature inert gas plasma MHD electrical power generator, which can be one of the candidates of space-based laser-to-electrical power converter, is examined by a time dependent two dimensional numerical simulation. In the present MHD generator, the inert gas is assumed to be ideally heated to about 10^4K pulsed-likely within short time (～1 μs) in a stagnant energy input volume, and the energy of high temperature inert gas is converted to the electricity with the medium of pure inert gas plasma without seeding. The numerical simulation results show that an enthalpy extraction ratio (= electrical output energy / pulsed heat energy) of several tens of % can be achieved, which is the same level as the conventional seeded non-equilibrium plasma MHD generator. Although there still exist many phenomena to be clarified and many problems to be overcome in order to realize the system, the pulsed heat source high temperature inert gas MHD generator is surely worth examining in more detail.

Introduction and Objective

Magneto-hydro-dynamic (MHD) electrical power generator is a device that directly converts the enthalpy of a high temperature gas to electric energy without any mechanical rotating high-temperature parts[1)]. In particular, a closed cycle MHD (CCMHD) electrical power generation system where the heat from the energy source is transferred to the inert gas as a working gas for the electrical power generation has a potential to meet the various kinds of energy sources. Since the system can have an attractive feature of a low specific mass below 1 kg/kWe, a nuclear electric propulsion system using the CCMHD energy conversion in space has been proposed[2)], which is based on the research and development in a highly efficient CCMHD power generation on the ground[3,4)]. In the generators of these CCMHD systems, generally the inert gas seeded with a small amount of alkali metal vapor flows continuously at a maximum gas temperature of about 2000K. In the past power generation experiments with a shock tunnel facility, an enthalpy extraction ratio (= electrical output power / pulsed heat power) over 30% has been successfully demonstrated[5)].

The MHD generator system which utilize CW or repetitively pulsed (RP) laser beam as a heat source, namely laser-driven MHD generator, has been

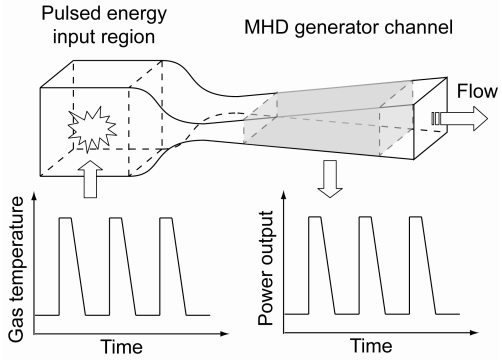

Figure 1. Schematic view of a pulsed heat source high temperature inert gas plasma MHD generator.

examined as a space-based laser-to-electrical power converter by several researchers in the past[6-8)]. Here the laser beams are regarded as an energy carrier in space. It has been suggested that this kind of MHD generator system should meet the requirements for the power converter from the viewpoints of 1) high energy-conversion efficiency, 2) high power density, 3) wavelength independence, 4) high power-to-weight ratio, 5) reliable and maintenance-free operation, and 6) not excessively expensive to manufacture. However, the studies of the laser-driven MHD generator have been restricted to some analytical investigations[6-8)], and the detail investigation, for instance the plasma - fluid dynamical behavior and performance, have not been done.

Therefore, a repetitively pulsed MHD generator is picked up in the present paper. As the first step of the study, the pulsed heat source is assumed to be input to the inert gas as an ideal heat source "q" instead of a specified heat source (for instance laser beam), although the generator performance surely depends on the energy transfer efficiency from the input (laser) energy to the gas energy. The authors have been called such an MHD generator "a pulsed heat source high temperature inert gas plasma MHD electrical power generator". In the present pulsed heat source MHD generator as shown in Fig 1, the inert gas (argon or helium) is assumed to be heated to about 10^4K pulsed-likely within short time (for instance 1 μs), the energy of high temperature inert gas is converted to the electricity with the medium of pure inert gas plasma without seeding. The pulsed heat energy is put repetitively into an upstream part of the MHD generator where a cold (room temperature)

inert gas flows continuously though the generator channel. That is, the high temperature inert gas plasma with high electrical conductivity for electrical power generation and the low temperature inert gas suitable for cooling the MHD generator channel flow alternately in an adequate duty factor in the generator. Therefore, the high generator performance can be obtained even under no seeding, pure inert gas condition, with keeping the time-averaged gas temperature below a tolerable value, although the electrical power generation is forced to be pulse-like or repetitive.

The authors have been studied the performance on a pulsed heat source MHD generator by using quasi-one dimensional numerical code[9]. In the paper, it is revealed that the enthalpy extraction ratio (output energy/input energy) of a pulsed heat source MHD generator can achieve 20-30%. However the multi-dimensional simulation has not been done. The energy input for instance by a pulsed laser should not be one dimensional but two dimensional at least, which is caused by the heating at the focused point. The objective of the present study, therefore, is to examine the generator performance and the plasma - fluid dynamical behavior in the pulsed heat source MHD generator by a time dependent two dimensional numerical simulations.

Numerical Procedure

Governing Equations

In the present numerical modeling, from the view of the engineering point, the conventional MHD approximations of the charge-neutrality and low magnetic Reynolds number are hired[10]. A simple two-temperature model is adopted for the non-equilibrium plasma, which consists of inert gas atoms, inert gas ions and electrons. The governing equations are conservation equations for MHD fluid flow and for charged particles, which are the same as those usually used for the numerical prediction of non-equilibrium plasma MHD generator[10]. The transport coefficients in viscosity or heat conduction term are evaluated by first Chapman-Enskog approximation[11].

MHD fluid flow

Continuity equation

$$\frac{\partial \rho}{\partial t} + \nabla \cdot (\rho \mathbf{u}) = 0 \qquad (1)$$

Momentum equation

$$\frac{\partial}{\partial t}(\rho \mathbf{u}) + \nabla \cdot (\rho \mathbf{u}\mathbf{u} + p) = \mathbf{j} \times \mathbf{B} + \nabla \tau_{ij} \qquad (2)$$

Total Energy equation

$$\frac{\partial E_s}{\partial t} + \nabla \cdot \{(E_s + p)\mathbf{u}\} = \mathbf{j} \cdot \mathbf{E} - \nabla \cdot \mathbf{q}_h - \nabla \cdot \mathbf{q}_e + \mathbf{u} \cdot \nabla \tau_{ij} + \Phi + q \qquad (3)$$

Charged Particles

Continuity equation of ion

$$\frac{\partial n_i^+}{\partial t} + \nabla \cdot (n_i^+ \mathbf{u}) = k_f n_i n_e - k_r n_i^+ n_e^2 \qquad (4)$$

Generalized Ohm's low

$$\mathbf{j} + \frac{\beta}{|\mathbf{B}|}(\mathbf{j} \times \mathbf{B}) = \sigma(\mathbf{E} + \mathbf{u} \times \mathbf{B} + \frac{\nabla p_e}{e n_e}) \qquad (5)$$

Electron energy equation

$$\frac{\partial U_e}{\partial t} + \nabla \cdot (U_e \mathbf{u}) = -p_e \nabla \cdot \mathbf{u} + \frac{|\mathbf{j}|^2}{\sigma} - \frac{\mathbf{j} \cdot \nabla p_e}{e n_e} - \frac{3}{2} k (T_e - T_g) n_e \sum_i \frac{2 m_e}{m_i} \nu_{ei} - \nabla \cdot \mathbf{q}_e + q \qquad (6)$$

where

$$p = (n_i + n_i^+) k T_g + p_e,$$
$$E_s = \rho(c_v T_g + \frac{1}{2}|\mathbf{u}|^2) + U_e, \qquad (7)$$
$$p_e = n_e k T_e,$$
$$U_e = n_e \frac{3}{2} k T_e + n_i^+ \varepsilon_i$$

The recombination rate coefficient kr in Eq. (4) is calculated according to Ref. 12. The hyperbolic equations above are solved by the Harten-Yee non-MUSCL type second-order upwind TVD scheme. The terms "q" of right hand side in Eq. (3) and (6) indicate an input power per unit volume from a pulsed heat source. The input power q is assumed to be absorbed uniformly in the inert gas of the energy input volume for an energy input time of 1 μs. The efficiency of the input energy and the inert gas is assumed as 100%. The time integrated value of input power q becomes the total input energy (for example 1J) and the time variation of input power q is assumed to be Gaussian in time. The electron number density is determined by Saha equation instead of Eq. (4) for the energy input time of 1 μs.

Working Condition

Fig 2 shows the calculation region in this study. Since the MHD generator is basically assumed as a linear shaped Faraday type MHD generator with infinite segmented electrodes, no Hall current is produced in Eq. (5). As typical values of the shape, the energy input volume is 4 x 4 x 10mm, the height of the throat is 1.0mm, the length of the electrode is 60mm, and the area ratio of the exit to the throat is 5. The energy input volume is determined as the high temperature inert gas suitable for MHD electrical power generation without seeding is produced for an energy input of 1.0 J/pulse (variable) under the initial conditions of a gas pressure of0.01 MPa and a gas temperature of 300K as typical values. The back pressure in the outlet of the MHD generator is set to 0.01MPa. The high temperature and high pressure inert gas produced by the pulsed heat source flows though the MHD generator channel with a sufficient electrical

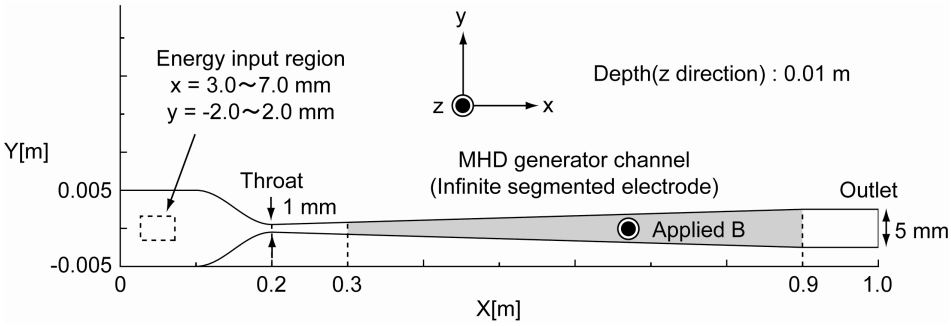

Figure 2. Calculation region.

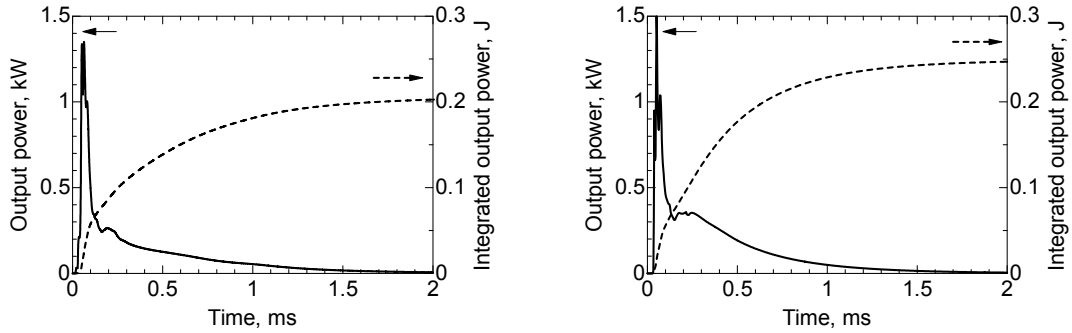

(a) Two dimensional simulation. (b) Quasi-one dimensional simulation.

Figure 3. Temporal evolutions of the output power and the integrated output power (input energy : 1 J, magnetic flux density : 4 T) in (a) two dimensional simulation, and (b) quasi-one dimensional simulation.

conductivity across a magnetic field. Although the generator shape is one of the important parameters for the generator performance, the optimization will be performed in the future work. Here, as for loading condition, a constant loading factor K of 0.5 is assumed at every location in the MHD generator channel. Thus, the electric field is given everywhere by the following equation and the load matching of the generator is not optimized in this study.

Loading factor

$$K = \frac{|\mathbf{E}|}{|\mathbf{u} \times \mathbf{B}|} = 0.5 \qquad (8)$$

Calculation Results

The calculation results are described from the viewpoint of 1) temporal evolutions of output power and plasma – fluid dynamical behavior, 2) dependence on input energy, and 3) dependence on magnetic flux density.

Temporal evolutions of output power and plasma – fluid dynamical behavior Fig 3 (a) shows the typical results of the temporal evolutions of the output power and the time integrated output power, that is, output energy for an input energy of 1.0 J/pulse (1 μs) and the initial working gas conditions (Ar, 0.01MPa, 300K). The magnetic flux density is set to 4T. The output power is generated during about 1.5 ms. The time integrated output power, that is, total output energy reaches 0.206J. When the enthalpy extraction ratio is defined as the ratio of total output energy to the input energy, the enthalpy extraction ratio is 20.6%. It should be noted that this value is almost the same level as the conventional seeded non-equilibrium plasma MHD generator, and is obtained under pure inert gas plasma without seed injection. Fig 3 (b) shows the results from a quasi-one dimensional simulation in order to compare with the two dimensional simulation result. The working conditions of the quasi-one dimensional simulation are the same as that of the two dimensional simulation. The time integrated output power and the enthalpy extraction ratio in the quasi-one simulation are 0.249J and 24.9%, respectively. It is seen that there are not essential difference between power output profile of the quasi-one and the two dimensional simulation, although the enthalpy extraction ratio in the two dimensional simulation is slightly lower than that in the quasi-one dimensional simulation. The output power has two peaks against time. The first peak around 0.05ms with high power and short duration is originated from the initial flow with relatively high electrical conductivity. The subsequent second peak around 0.2ms with low power is attributed to a quasi-steady flow from the stagnant energy input volume. It is noted that the maximal enthalpy extraction ratio of the present generator is expected to be higher than 24.9% or

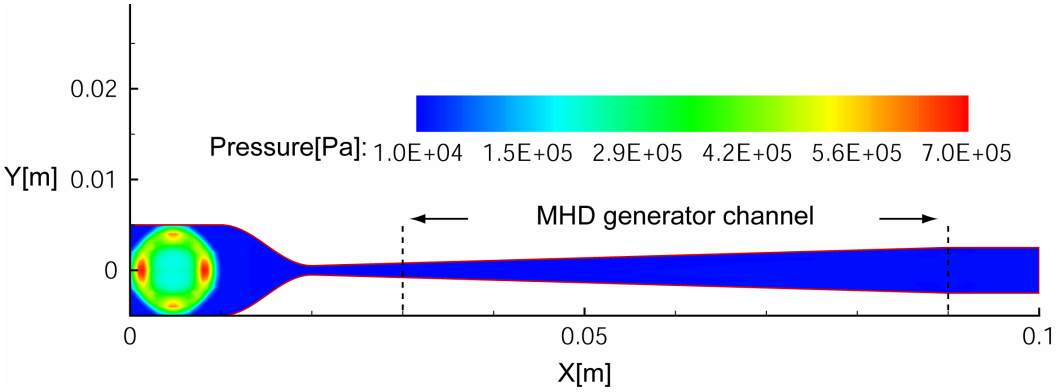

(a) Pressure distribution at t = 0.75 μ s.

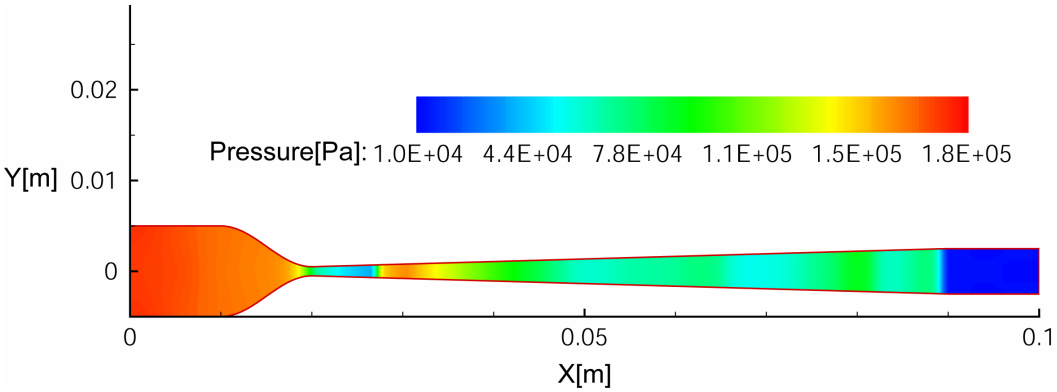

(b) Pressure distribution at t = 65 μ s around first peak of output power profile shown in Fig 3.

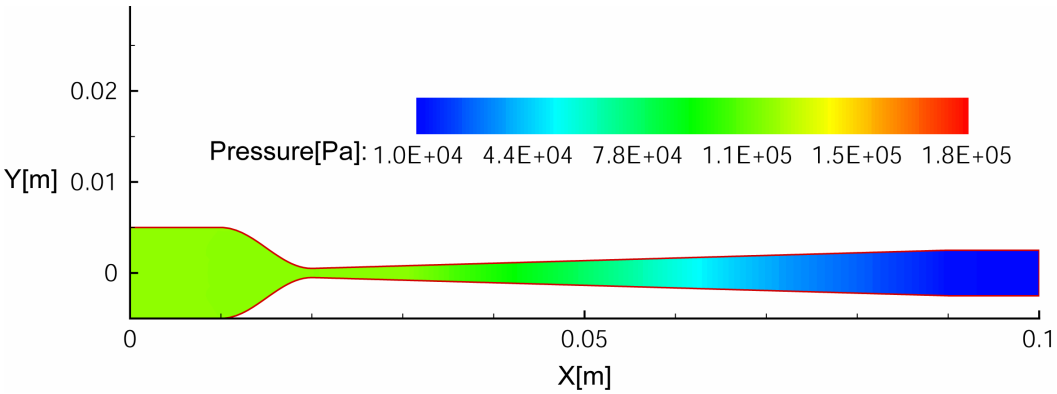

(c) Pressure distribution at t = 210 μ s around second peak of output power profile shown in Fig 3.

Figure 4. Temporal evolutions of pressure distribution. pressure distribution after (a) 0.75 μ s, (b) 65 μ s , (c) 210 μ s, from the energy input end, respectively. (input energy : 1 J, magnetic flux density : 4 T)

20.4% shown in Fig 3 (a), (b), if the load matching of the generator is optimized.

Fig 4 (a)-(c) and Fig 5 (a)-(c) show the temporal evolutions of Mach number distribution and the temporal evolutions of pressure distribution after (a) 0.75 μ s, (b) 65 μ s around first peak of output power, and (c) 210 μ s around second peak of output power from the energy input end, respectively. These figures correspond to the output shown in Fig 3. At first, the shockwave is generated around x = 0-0.01m due to the production of high pressure and high temperature inert gas in the energy input region (Fig 4, 5 (a)). The relations between the input energy and the plasma properties generated by energy input are shown later. When the shockwave propagation at the initial stage reaches the outlet of the generator channel, the first peak of the output power shown in Fig 3 appears (Fig 4, 5 (b)). Although the initial flow generated by energy input has low electrical conductivity, the Mach number (flow velocity) of that is relatively high in the generator channel. Then the Mach number in the

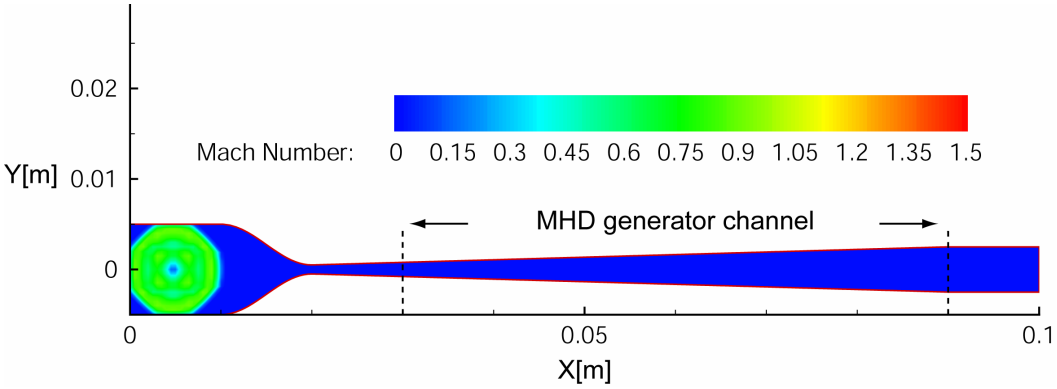

(a) Mach number distribution at t = 0.75 μ s.

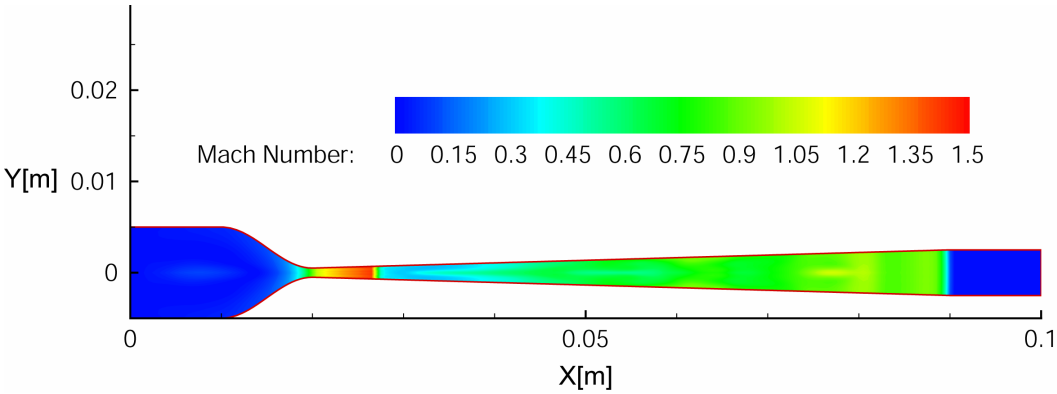

(b) Mach number distribution at t = 65 μ s around first peak of output power profile shown in Fig 3.

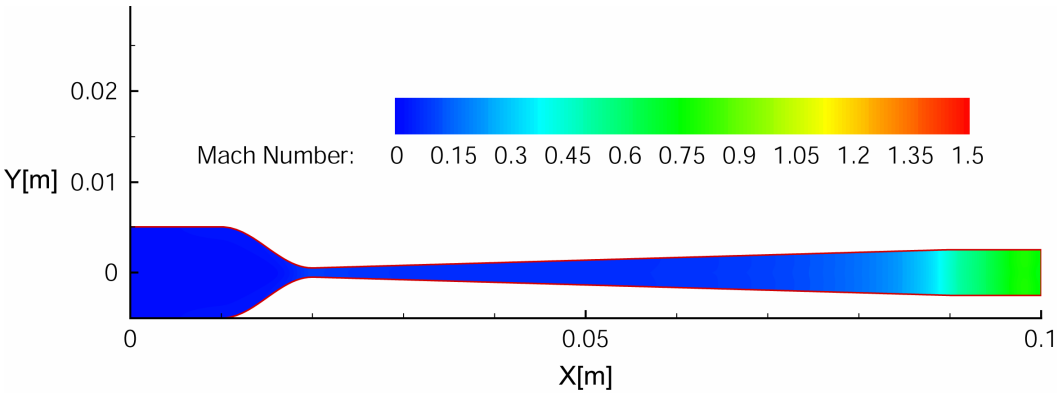

(c) Mach number distribution at t = 210 μ s around second peak of output power profile shown in Fig 3.

Figure 5. Temporal evolutions of Mach number distribution. Mach number distribution after (a) 0.75 μ s, (b) 65 μ s , (c) 210 μ s, from the energy input end, respectively. (input energy : 1 J, magnetic flux density : 4 T)

channel is about 0.5-1.0. After the peak time 65 μ s of the output power, the plasma with the high electrical conductivity expands in the whole region of the generator. When the fluid behavior in the generator becomes almost quasi-steady flow, the second peak of power generation appears (Fig 4, 5 (c)). The reason for the low power at around second peak is the decrease in the Mach number owing to the strong MHD interaction. It is noted that the pressure distribution shown in Fig 5 (c) depend not on y direction but on x direction, Moreover, the Mach number becomes subsonic in the whole region of the generator as shown in Fig 5 (c), although there exist the throat. Then the Mach number is about 0.1 and does not choke at the throat.

It should be noted in Fig 4 and 5 that the plasma and fluid flow in the MHD generator seems to be rather one dimensional, although the high pressure and temperature gas is expanded two dimensionally in the

Table 1 Working gas conditions in the energy input volume after the energy input
Initial conditions: Ar, 0.01MPa, 300K, 4mmx4mmx10mm

Input energy [J]	0.1	0.3	0.5	0.8	1.0
static gas pressure p (MPa)	0.355	0.545	0.696	0.991	1.27
static gas temperature T_g (=T_e) (K)	10500	13900	15600	17800	19700
total energy per unit volume E_s (MJ/m^3)	0.64	1.89	3.14	5.02	6.26
electron pressure p_e (MPa)	0.00618	0.0815	0.178	0.397	0.605
electron energy per unit volume U_e (MJ/m^3)	0.118	1.19	2.36	4.12	5.27
electrical conductivity σ (S/m)	1740	3560	4490	6150	7590

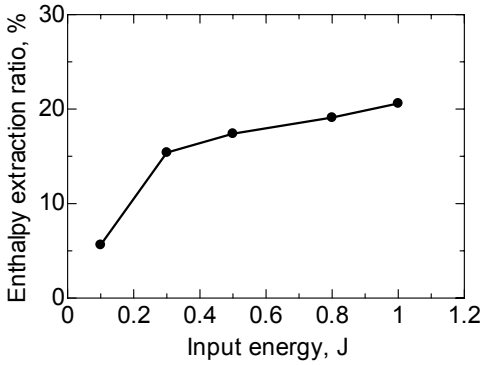

Figure 6. Dependence on input energy. (magnetic flux density : 4 T)

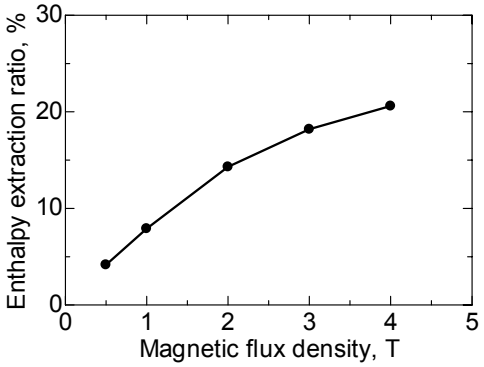

Figure 7. Dependence on magnetic flux density. (input energy : 1 J)

stagnant volume including the energy input region at the energy input (0.75 μ s).

Dependence on input energy In this section, the effects of the input energy on the performance of the pulsed heat source high temperature inert gas plasma MHD generator are examined. The input energy strongly affects initially produced high temperature and high pressure working gas conditions in the energy input volume. Table 1 shows the values of static gas pressure p, static gas temperature T_g, total energy per unit volume E_s, electron pressure p_e, electron energy per unit volume U_e, electrical conductivity σ after the energy input (1 μs, Gaussian in time) with different values of the input energy. The input energy is fed into the electron energy at first, and then the electron temperature increases steeply. The electron energy is consumed with the progress of the ionization and the increase in the gas temperature through collisions with heavy particles. Since there is no energy gain and loss after the energy input, the electron temperature decreases and the gas temperature increases, and eventually these temperatures have the same value. Then the electron number density coincides with the value derived from the Saha equilibrium for the temperature. The gas properties can change almost at constant volume. That is, roughly, the increase in the gas pressure is proportional to the increase in the gas temperature, although electron energy (electron pressure) can not be ignored. As a typical case, the initial gas (argon) under a pressure of 0.01MPa and a temperature of

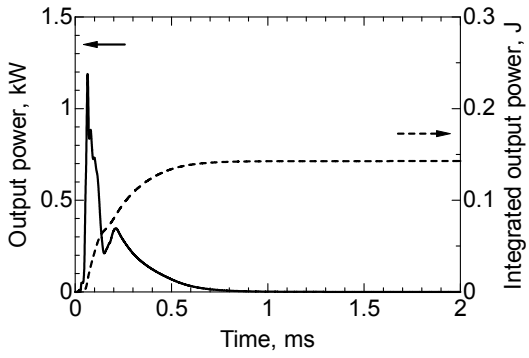

Figure 8. Temporal evolutions of the output power and the integrated output power. (input energy : 1 J, magnetic flux density : 2 T)

300K is pressurized to 1.27MPa and heated to 19,700K for an input energy of 1.0J. As shown in Table 1, the typical values of gas properties in the energy input volume are in the range of 0.5-1.3MPa and 14,000-20,000K in the present study.

Fig 5 shows the enthalpy extraction ratio against the input energy. It is noted here that the enthalpy extraction ratio increases and tends to saturate with the input energy. Generally the enthalpy extraction ratio does not so depend on the input energy (thermal input) for the conventional seeded non-equilibrium plasma MHD generator. Thus, the increase in the enthalpy extraction ratio with the input energy in the pulsed heat source MHD generator is originated from the

nonlinear increase in the electrical conductivity with the electron temperature, as shown in Table 1, although the electrical conductivity shown there is the value not in the generator region but in the energy input volume. Judged from Fig 6, the enthalpy extraction ratio seems to saturate around an input energy of 0.3-1.0J. The numerical simulation results show that the increase in the output energy for the input energy is attributed to the relatively higher electrical conductivity in the generator region, whereas there is no big difference in the velocity. As is seen in Table 1, with the increase in the input energy, the large part of input energy is distributed to the electron energy; on the contrary, the gas temperature tends to be almost constant, leading to the saturation of the gas velocity. As a result, the output power increases roughly corresponding to the increase in the input energy, and the enthalpy extraction ratio does not change so much.

Dependence on magnetic flux density The applied magnetic flux density is one of the important parameters for the improvement in the generator performance, because the power density is locally proportional to $\sigma u^2 B^2$ for an MHD generator. Fig 7 shows the enthalpy extraction ratio for different magnetic flux densities. It is found obviously that the enthalpy extraction ratio increases with the magnetic flux density. However the enthalpy extraction ratio seems to saturate against the magnetic flux density. This is attributed to the decrease in the gas velocity under the strong Lorentz force. Fig 8 shows the temporal evolutions of the output power and the integrated output power under the condition of applied magnetic flux density 2T. In this case, as well as the case of 4T (Fig 3), the power output profile has two peaks against time. The first peak appears around 0.05ms and the second one appears around 0.2 – 0.3ms as shown in Fig 8. Here, it is seen that the second peak is enhanced relatively in comparison with the case of 4T, although the first peak is smaller. The duration of power generation is also shorter than the case of 4T. When the flow in the generator becomes quasi-steady state, this second peak appears. The remarkable appearance of the second peak is attributed to the decline of induced Lorentz force associated with the decrease in the magnetic flux density, in consequence, Mach number in the generator channel and output power around second peak increase compared with the case of 4T.

Nomenclature

$\mathbf{B}$ = magnetic flux density
C_v = specific heat at constant volume
$\mathbf{E}$ = electric field
E_s = total energy per unit volume
e = elementary electric charge
$\mathbf{j}$ = current density
k = Boltzmann constant
K = loading factor
k_f = ionization rate coefficient
k_r = three body recombination rate coefficient
m_i = mass of ith particle (i=electron, neutral atom, ion)
n_i = number density of ith particle (i=electron, neutral atom)
n_i^+ = number density of ion (= n_e)
p = static gas pressure
p_e = electron pressure
q = pulsed input power from pulsed heat source
$\mathbf{q}_e$ = electron heat flux
$\mathbf{q}_h$ = heavy particle heat flux
T_g = static gas temperature
T_e = electron temperature
U_e = electron energy per unit volume
$\mathbf{u}$ = gas velocity
ε_i = ionization energy of ion
ν_{ei} = collision frequency for electron with ith particle
ρ = density
σ = electrical conductivity
τ_{ij} = viscous stress tensor
Φ = dissipation function

Conclusion

The performance and the plasma – fluid dynamical behavior in the pulsed heat source high temperature inert gas plasma MHD electrical power generator is examined by a time dependent two dimensional numerical simulation.

1) The enthalpy extraction ratio (the ratio of total output energy to the input energy) of the pulsed heat source MHD generator can reach 20% without seed injection even if the load matching of the generator is not optimized. The output power profile has two peaks against time. The first peak with high power is originated from the initial flow with high electrical conductivity, and the subsequent second peak with low power is attributed to a quasi-steady flow from the stagnant energy input volume. During the power generation, the flow in the generator mainly becomes subsonic owing to the induced strong Lorentz force.
2) The plasma and fluid flow in the MHD generator seems to be rather one dimensional, although the high pressure and temperature gas is expanded two dimensionally in the stagnant volume including the energy input region at the energy input. There is no marked difference in the temporal evolutions of the output power and the time integrated output power between quasi-one and two dimensional simulations..

3) The enthalpy extraction ratio increases and tends to saturate with the input energy. The increase in the enthalpy extraction ratio is originated from the nonlinear increase in the electrical conductivity with the input energy.

4) The enthalpy extraction ratio increases and tends to saturate with the magnetic flux density. When the magnetic flux density decreases, the second peak of the output power profile becomes high significantly compared with the case of high magnetic flux density. The remarkable appearance of the second peak is

attributed to the decline of induced Lorentz force associated with the decrease in the magnetic flux density.

Although there still exist many phenomena to be clarified and many problems to be overcome in order to realize the system, the pulsed heat source high temperature inert gas plasma MHD electrical power generator is surely worth examining in more detail. As a future plan, the simulation with taking account of the energy transfer from the input energy (for instance, laser energy) to the working gas energy should be done. Furthermore, the configuration and performance of the power generation system including the quasi-stationary cyclic operation in the pulsed heat source MHD electrical power generator should be established.

References

1) Rosa, R. J.: *Magnetohydrodynamic Energy Conversion, Revised Printing*, Springer-Verlag, New York, 1987.
2) Litchford, R. J., Bitteker, L. and Jones, J.: Prospects for Nuclear Propulsion Using Closed-Cycle Magnetohydrodynamic Energy Conversion, 39th AIAA Aerospace Sciences, AIAA-2001-0961, 2001.
3) Okuno, Y., Okamura, T., Murakami, T., Ohgaki, K., Takahashi, H. and Yamasaki, H.: Construction of Closed Loop Facility for CCMHD Power Generation, 34th Plasmadynamics and Lasers Conference, AIAA-2003-4280, 2003.
4) Liberati, A., Murakami, T., Okuno, Y. and Yamasaki, H.: Numerical simulation of Performance of Disk MHD Generator in the Closed Loop Experimental Facility, *IEEE Trans. Plasma Science*, **34** (6), 2006, pp.2669-2677.
5) Murakami, T., Okuno, Y. and Yamasaki, H.: Achievement of the Highest Performance of a CCMHD Generator: an Isentropic Efficiency of 63% and an Enthalpy Extraction Ratio of 31%, *IEEE Trans. Plasma Science*, **32** (5), 2004, pp.1886-1892.
6) Jalufka, N. W.: Laser Production and Heating of Plasma for MHD Application, NASA TP-2798, 1988.
7) Maxwell, C. D. and Myrabo, L. N.: Feasibility of Laser-Driven Repetitive-Pulsed MHD Generation, AIAA-83-1442, 1983.
8) Choi, S. H.: Space-Based Laser-Driven MHD Generator: Feasibility Study, NASA CR-178184, 1986.
9) Kajihara, S., Matsumoto, M., Murakami, T. and Okuno, Y.: Numerical Study of Pulsed Heat Source MHD Electrical Power Generation, 37th Plasmadynamics and Lasers Conference, AIAA-2007-4245, 2007.
10) Mitchner, M. and Kruger, C. H.: *Partially Ionized Gases*, John Wiley & Sons, New York, 1973.
11) Hirschfelder, J. O., Curtiss, C. F. and Bird, R. B.: *Molecular Theory of Gases and Liquids*, John Wiley & Sons, New York, 1967
12) Owano, T. G. and Kruger, C. H.: Electron-Ion Three-body Recombination Coefficient of Argon, *AIAA Journal*, **31** (1), 1993, pp.75-82.